CARBON 47 (2009) 3452–3460

available at www.sciencedirect.com

ScienceDirect

journal homepage: www.elsevier.com/locate/carbon

Electric field induced reversible switch in hydrogen storage based on single-layer and bilayer graphenes

W. Liu [a,b], *Y.H. Zhao* [a], *J. Nguyen* [a], *Y. Li* [a], *Q. Jiang* [b,*], *E.J. Lavernia* [a,*]

[a] *Department of Chemical Engineering and Materials Science, University of California, Davis, CA 95616, United States*
[b] *Key Laboratory of Automobile Materials, Ministry of Education, and School of Materials Science and Engineering, Jilin University, Changchun 130022, China*

ARTICLE INFO

Article history:
Received 7 January 2009
Accepted 7 August 2009
Available online 13 August 2009

ABSTRACT

In an ideal hydrogen storage system, binding strength should increase during adsorption whereas the opposite should be the case during desorption. These two seemingly contradictory requirements limit the types of systems that can be utilized. Density-functional theory (DFT) calculations are carried out to investigate hydrogen physisorption on Li-doped single-layer and bilayer graphenes. We propose that the superimposition of an electric field can be used to effectively control hydrogen adsorption. More specifically, we report that hydrogen binding can be enhanced under a positive electric field, whereas it can be weakened under a negative electric field. Our results show that the binding strength increases by 88% when a field with a magnitude of +0.020 au is imposed. Hirshfeld charge analysis results suggest that an increase in the binding strength will occur as long as the Li (or C) carries more positive (or negative) charges. Our calculations demonstrate that, in the case of Li-doped graphene, the application of a positive electric field yields an increase in binding strength during adsorption while a negative field decreases the binding strength during desorption.

1. Introduction

Environmentally, hydrogen is of interest as a clean energy source since it does not create air pollution or generate greenhouse gas emissions [1]. One of the key challenges that needs to be overcome before the so-called hydrogen fuel economy becomes a reality is how to store hydrogen safely and economically [2,3]. Initial interest in metal hydrides, such as $LaNi_5H_6$ was dampened by their low gravimetric capacity ($\sim$1.4 wt.%) and high cost [4]. More recently, lightweight carbon-based nanostructures (including nanotubes, fullerene, nanofibers, and graphene) have emerged as attractive hydrogen storage materials, partly because of their high surface-volume ratio [5]. Among these different forms of carbon, the properties of the recently discovered graphene phase represent a quandary. On one hand, its super-high strength and unusual electronic properties are attractive properties for a hydrogen storage media [6–8]. On the other hand, their flat surfaces may adsorb fewer hydrogen molecules than those corresponding to structures with curvatures, such as nanotubes [9]. Since relatively large graphene sheets, up to 100 μm in size, have been successfully synthesized [10], the hydrogen storage behavior of graphene is actively being studied and compared to those of carbon nanotubes and fullerenes [11–13].

In cases when hydrogen is chemisorbed in atomic form, the transition from sp^2 to sp^3 hybridization is widely accepted as the mechanism responsible for carbon hydrogenation [14]. In this case, large binding strengths can be achieved between C–H, with adsorption energy E_{ad} values on the order of -0.67

---

[*] *Corresponding authors:* Fax: +86 431 85095876 (Q. Jiang), fax: +1 530 752 8058 (E.J. Lavernia).
E-mail addresses: jiangq@jlu.edu.cn (Q. Jiang), lavernia@ucdavis.edu (E.J. Lavernia).

0008-6223/$ - see front matter © 2009 Elsevier Ltd. All rights reserved.
doi:10.1016/j.carbon.2009.08.012

to −0.77 eV/H atom [15,16]. The magnitude of these binding strength values can be decreased to −2.13 eV/H atom, by doping two boron atoms in the graphene sheets [17]. However, a strong binding strength will be detrimental when hydrogen release is required [18]. Hence, physisorption and chemisorption of molecular hydrogen represent more viable mechanisms for hydrogen storage applications [19]. The main challenge is that the binding between hydrogen and graphene is quite weak (merely on the order of −0.10 eV/H_2), which effectively yields a low storage capacity [20–22]. Therefore, the attainment of moderate adsorption energy has remained a challenge, either due to weak physisorption or, at the other extreme, due to strong chemisorption that renders hydrogen release difficult. More recently, a few novel approaches have been proposed to enhance the storage ability of graphene-based systems. For example, by doping the graphene with Li, the binding strength increased twofold ($E = -0.184$ eV/H_2) over that of the undoped material [20]. Similarly, Ti decoration reportedly increased the hydrogen storage capacity of graphene, where up to four molecules can be adsorbed around per adatom [23]. In related work, it was reported that Li and Ti atoms can be adsorbed on graphene forming an uniform and stable coverage on both sides, which can serve as a high-capacity hydrogen storage media [12,24]. Noteworthy is the recent report of a novel storage model comprised of three-dimensional pillared graphene [25]. Although this material was anticipated to reach the volumetric target of the US Department of Energy (45 g/l for mobile applications), fabrication issues have precluded experimental verification. In the cases reviewed here, the mechanism responsible for the increase in hydrogen physisorption energy involved enhanced charge transfer from the metallic dopants to the carbon-based nanostructures [20,26].

In light of the above discussion, we hypothesize that the imposition of an electric field on Li-doped graphene, can be used to control the binding strength during adsorption and desorption. There appears to be some support to this hypothesis, since the imposition of an electric field has been proven to be an effective approach to redistribute charges [27–30]. In particular, graphene has been shown to exhibit a pronounced response to a perpendicular external electric field due to its high electronic behavior [10]. A notable fact is that in addition to studies on single-layer graphene, prior experiments indicated that bilayer graphenes are also very sensitive to the presence of electric fields [6,31]. For example, the electronic gap of a bilayer graphene can be controlled externally by applying a gap tunable by the electric field [32]. In addition, angle-resolved photoemission results showed that an electric field is associated with the charge transfer from dopants to the carbon atoms in a K-doped graphene bilayer [33]. Based upon these findings, both single-layer and bilayer graphenes will be chosen as prototypes in our calculations; inspection of the scientific literature fails to reveal prior studies on bilayer graphenes. Since the directions of the imposed fields can readily be altered, we can not only increase the bonding in the adsorption process, but also decrease it in the desorption process. In this case, the electric field effectively yields a "reversible switch" for hydrogen storage.

In this contribution, Li-doped single-layer and bilayer graphenes are utilized as hydrogen storage models. External electric fields, with different intensities and orientation are superimposed into the relaxed systems. The variations of the hydrogen binding strengths are compared in terms of their corresponding adsorption energy E_{ad} values. In addition, charge redistribution behavior is discussed based on Hirshfeld charge analysis.

2. Computational framework

In this study, all calculations were performed using the spin-polarized first-principle method as implemented in the DMol^3 code [34,35]. Exchange–correlation functions were computed within a local density approximation (LDA) with the Perdew–Wang–correlation (PWC) throughout the paper [36]. This strategy was adopted because the strong sp^2 bonds inside graphene layers can be accurately described by the LDA approach [24,37]; moreover, the physisorption results calculated by LDA are in good agreement with experimental results [20,38]. In this work, the H_2/Li/graphene system was selected as a model material to test the rationality of the functional. Our LDA calculations predicted that a single H can be adsorbed by the Li-doped graphene with $E = -0.153$ eV/H_2, which agrees with previous theoretical and experimental results [20,39,40]. In contrast, the generalized gradient approximation (GGA) with Perdew–Wang 91 (PW91) functional [41] produced a purely repulsive interaction between H and the storage media (a similar GGA result has also been reported for the H/graphene system [42]), which is contradictory to the widely accepted conclusion that graphene functionalized by Li atoms enhances H storage capacity [20,24]. All electrons were chosen as the core treatment method and a double numeric basis with polarization set was adopted as the basis set [34]. Since the obtained results are very sensitive to the accuracy settings under the electric fields, the k-point was set to $8 \times 8 \times 1$ for all the slab models, the real-space global orbital cutoff radius was chosen to be as high as 6.0 Å, and smearing was 0.002 Ha. Each atom in the storage models was allowed to relax without any constraints.

A uniform (2×2) graphene supercell was established with an in-plane lattice parameter of 4.920 Å. In the case of the single-layer model, graphene is a planar sheet of sp^2-bonded carbon atoms that are densely packed in a honeycomb crystal lattice, as seen in Fig. 1. Although different doping sites were considered, our calculations showed that the most stable position for Li is above the center of a hexagonal carbon [24]. The equilibrium distance between Li and the graphene layer is determined to be 1.747 Å, which is consistent with other theoretical results [20]. For comparison purposes, the above system was recalculated by the GGA functional. In this case, the distance increased to 1.870 Å, since LDA overbinds atoms when it is compared with GGA. In the case of the bilayer model, two graphene monolayers are stacked in the natural graphite order with an interlayer space of 3.268 Å (see Fig. 2). After relaxation, the Li–graphene distance is 1.671 Å and the metal atom position remains above the center of a carbon ring. A vacuum thickness of 20 Å was employed along the z direction of the carbon sheets to avoid the interactions from neighboring molecules. Three initial hydrogen adsorption sites were considered around the dopant: (1) Atop Parallel

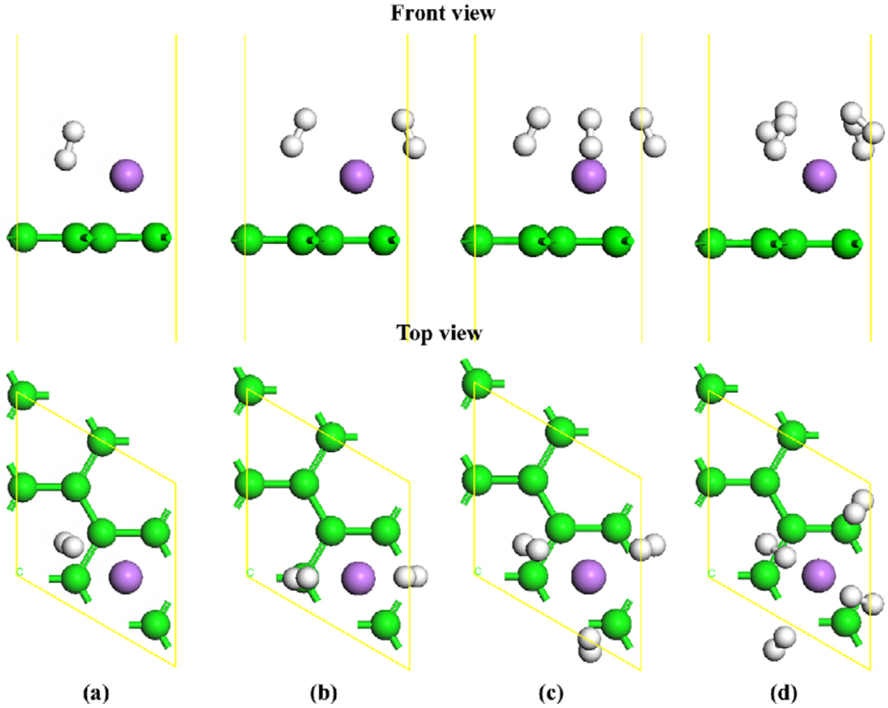

Fig. 1 – The relaxed hydrogen storage systems based on the Li-doped single-layer graphene. The plots a–d show the relaxed models when hydrogen number increases from 1 to 4. The white, purple, and green spheres represent H, Li, and C atoms, respectively. (For interpretation of the references to colour in this figure legend, the reader is referred to the web version of this article.)

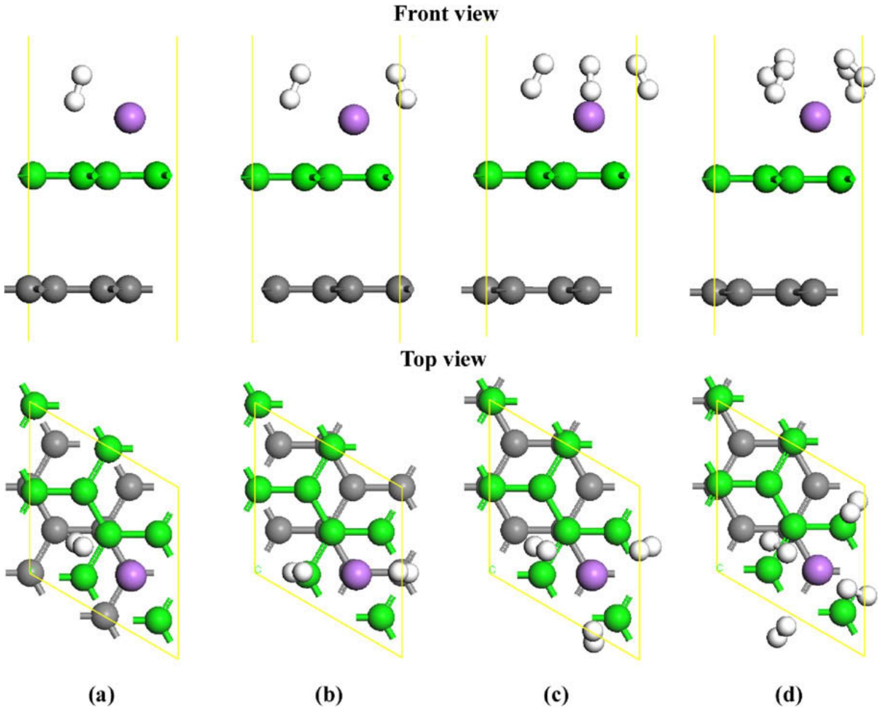

Fig. 2 – The relaxed hydrogen storage systems based on the Li-doped bilayer graphene. The plots a–d show the relaxed models when hydrogen number increases from 1 to 4. The white, purple, and green spheres represent H, Li, and C atoms, respectively. (For interpretation of the references to colour in this figure legend, the reader is referred to the web version of this article.)

site (AP: hydrogen lies above a Li atom and parallel to the carbon sheet); (2) Bridge Parallel site (BP: hydrogen located besides a Li atom and parallel to the carbon sheet); and (3) Bridge Vertical site (BV: hydrogen located besides a Li atom and vertical to the carbon sheet). Considering a stable system can store a maximum of four molecules [24], the hydrogen number increased gradually from one to four in our storage systems, as shown in Figs. 1 and 2. Electric fields with a field intensity of $F = \pm0.020$ au were applied perpendicular to the carbon atom planes, in the upward (defined as "+") or downward (defined as "−"). The $E_{ad}(F)$ values are indicative of the adsorption energy obtained under the intensity field F. In this case, the energy of the fragments should also be obtained in presence of the external F [43]. Thus,

$$E_{ad}(F) = [E_F(nH_2 + Li + C_m) - E_F(Li + C) - nE_F(H_2)]/n, \qquad (1)$$

where n and m indicates the numbers of hydrogen molecules and C atoms, respectively. The physical storage mechanism is primarily physisorption with van der Waals forces in nature, thus hydrogen maintains its molecular identity [44]. The negative value of E_{ad} indicates that the adsorption is exothermic, hence stable [45]. To further study the intensity-dependent behavior, a series of fields with $F = +0.020$, $+0.015$, $+0.010$, 0.000, -0.010, -0.015, and -0.020 au were imposed on the $2H_2$ adsorbed bilayer graphenes. The field-induced changes in electronic properties were determined by Hirshfeld population analysis and Density of States (DOS) plots.

3. Results and discussion

We first address the E_{ad} values for single-layer graphene in the absence of a field. It is readily seen from Table 1 that our calculated results agree nicely with those in [24], except for the case of the one-H_2 adsorption system. In this study, the hydrogen molecule was found to lie on top of the Li dopant (i.e. AP site here) with $E_{ad} = -0.09$ eV/H_2 [24]. However, we revisited all three hydrogen adsorption sites and obtained $E_{ad} = -0.153$, -0.107, and -0.076 eV/H_2 for the BV, BP, and AP, respectively. Thus, BV here should be more stable than AP and BP sites, where hydrogen is vertical to a C–C bond besides the Li, as shown in Fig. 1a. In fact, our value of $E_{ad} = -0.153$ eV/H_2 is close to another literature datum of $E_{ad} = -0.184$ eV/H_2 [20]. Similar configurations can be achieved when two or more hydrogen molecules are introduced. As shown in plots b–d of Fig. 1, all relaxed H–H bonds tilt at the bridge site and located symmetrically around the Li dopant, which is consistent with the corresponding geometries reported in literature [24]. The average E_{ad} value increases slightly as n increases, where $E_{ad} = -0.225$, -0.219, and -0.197 eV/H_2 for the $2H_2$, $3H_2$, and $4H_2$-adsorbed systems, respectively. Given the weak binding strength of -0.09 eV/H_2 for hydrogen on pristine graphene [20–22], the hydrogen storage ability of graphenes can indeed be significantly enhanced via Li doping.

Now we address the binding results in the presence of an electric field. As listed in Table 1, the E value for the H_2/Li/single-layer graphene decreases dramatically to -0.288 eV/H_2 under $F = +0.020$ au. This value is almost twice that of $E_{ad} = -0.153$ eV/H_2 in the absence of a field and is a factor of two lower than $E_{ad} = -0.09$ eV/H_2 on pristine graphene [20–22]. For comparison purposes, the above system was recalculated using the GGA–PW91 functional. From Table 1, the determined $E_{ad} = -0.154$ eV/H_2 from GGA compared to -0.288 eV/H_2 as determined from LDA, is almost twice as large. As mentioned above, GGA predicts that H_2 cannot be stably adsorbed without a field. Therefore, the negative E value under +0.020 au further confirms that a positive field can evidently enhance the interactions between H and the Li-doped graphene. Similarly, the E value decreases from -0.225 (or -0.219) to -0.288 (or -0.277) eV/H_2 in the case of two (or three) molecules, leading to an approximate 30% binding enhancement. Nevertheless, the $4H_2$/Li/single-layer graphene seems to be "insensitive" to the presence of external fields. To explain this phenomenon, a Hirshfeld charge analysis was carried out for this system, and the results showed that Li carries a +0.191 e charge in the absence of the field. This value only increases to +0.208 e when $F = +0.020$ au. Since only a 2.23% charge variation can be detected for each hydrogen, it is safe to argue that the field indeed has a limited influence on the 4H system. In contrast, opposite binding trends are observed when $F = -0.020$ au. As listed in Table 1, $E_{ad} = -0.110$, -0.101, -0.184, and -0.192 eV/H_2 in the cases of one, two, three,

Table 1 – Calculated average $-E_{ad}(F)$ values in eV/H_2 for the Li-doped single-layer and bilayer graphenes, with hydrogen numbers n increased from 1 to 4. Other simulated results are also listed for a comparison purpose.

Li/graphenes	n	$F = 0.000$ au		$F = +0.020$ au		$F = -0.020$ au	
		$-E_{ad}$	Other [24]	$-E_{ad}$	$\Delta_+\%$[b]	$-E_{ad}$	$\Delta_-\%$[b]
Single-layer	1	0.153	0.09[a] 0.184 [20]	0.288[c]	+88.24	0.110	−28.11
	2	0.225	0.22	0.288	+28.00	0.101	−55.11
	3	0.219	0.21	0.277	+26.48	0.184	−15.98
	4	0.197	0.20	0.201	+2.10	0.192	−2.54
Bilayer	1	0.188		0.294	+56.38	0.131	−30.32
	2	0.244		0.295	+20.90	0.105	−56.97
	3	0.230		0.285	+23.91	0.165	−28.26
	4	0.202		0.212	+4.95	0.194	−3.96

a This -0.09 eV/H_2 corresponds to the AP site, which is close to our 0.076 eV/H_2 for the AP site.

b Δ% indicates the percent change of the E_{ad} values induced by fields, where the subscripts + and − indicate the positive and negative fields, respectively.

c $E_{ad} = -0.154$ eV/H_2 when the GGA–PW91 functional is used.

and four molecules. The negative field results in a 2.54–55.11% binding strength decrease as compared to the cases in the absence of a field. Therefore, the imposition of a negative field is beneficial to the release of a hydrogen molecule.

To understand the above *E* variations induced by the presence of an electric field, Hirshfeld charge analysis was carried out for the H_2/Li/single-layer graphene. As listed in Table 2, the charge Li carried in the H_2-free system increases significantly (nearly doubled) from +0.219 when $F = 0.000$ au to +0.417 *e* when $F = +0.020$ au. In contrast, the charges C(1) and C(4) carried decrease from −0.014 to −0.037 *e*, and the remaining C atoms decrease from −0.032 to −0.057 *e*. These results make physical sense, since the electrons will move downward from Li to the carbon sheet after the superimposition of an upward field. Since Li is more positive and graphene is more negative, $F = +0.020$ au renders an extra dipole moment and thus enhances the hydrogen adsorption. After adsorption, it is readily seen from Table 2 that the molecule obtains 0.003 *e* whereas Li loses 0.043 *e* in the absence of a field. This is consistent with results from a prior study which show that H atoms receiving a charge from Li become negatively charged and the covalent H–H bond becomes polarized [24]. In contrast, both H(1) and H(2) become cations and the charge of Li decreases from +0.417 to +0.334 *e* when $F = +0.020$ au. These results are attributed to the downward charge transfer (from H_2 to Li) in the presence of a positive field. Note that although many methods in prior studies have been proposed to enhance the charge transfer, the original idea introduced in this paper, namely the imposition of an electric field, should represent a breakthrough in hydrogen storage.

For the case when $F = -0.020$ au field is imposed, the charge Li carried decreases significantly from +0.219 to +0.033 *e*, as shown in Table 2. The corresponding charges carried by C are approximately zero, ranging from −0.009 to +0.007 *e*. This charge redistribution is evidently attributed to the upward charge transfer induced by a negative field. Since the ionizations of both Li and C have decreased considerably, the hydrogen binding will be weakened and this is presumably the reason why a negative field facilitates the release of hydrogen. In contrast to the cases when $F = 0.000$ and +0.020 au, a notable point is that C(1) and C(4) become cations while the remaining C atoms continue to be anions when $F = -0.020$ au. Thus, the ionization might be further degenerated since the influence from C atoms may counteract each other in the graphene sheet. In addition, the adsorbed C(5) and C(6) atoms always carry the same amount of charges, which are located symmetrically beside the adsorbed hydrogen molecule.

Similar to the situations in the single-layer systems, Li transfers a portion of its charge to bilayer graphene and thus carries +0.245 *e* in the absence of a field. Three possible hydrogen adsorption sites were considered when a hydrogen molecule is adsorbed, and the corresponding $E_{ad} = -0.188$, −0.139, and −0.115 eV/H_2 for the BV, BP, and AP sites, respectively. Hence, BV is also the most preferable site for the H_2/Li/bilayer graphene system. The average $E = -0.244$, −0.230, and −0.202 eV/H_2 when *n* increases from 2 to 4. The relaxed hydrogen geometries on the single-layer graphene (see Fig. 1) and bilayer graphene (see Fig. 2) are very close to each other. In fact, regardless of the initial molecular configurations, the same finial structures are achieved. Since all hydrogen molecules are tilted after full relaxation, one of the two H atoms of each adsorbed hydrogen molecule becomes relatively closer to the Li dopant [24].

Comparing the E_{ad} data in Table 1, we can note that bilayer graphene has a slightly stronger binding strength than that of the single-layer graphene system. For example, $E_{ad} = -0.153$ eV/H_2 for the H_2/Li/single-layer graphene is 22.88% larger than $E_2 = -0.188$ eV/H_2 for the H_2/Li/bilayer graphene. Fig. 3a can be used to explain this phenomenon, in which not only the C atoms in the upper layer, but also those in the lower layer carry negative charges, although the amount is quite small (merely around −0.005 to −0.006 *e*). Since both of these two layers can "adopt" charges, the Li dopant is more ionized on the bilayer graphene. The above results can also be visualized in the plots of electron density differences. As

Table 2 – Hirshfeld charge analysis for the single-layer graphene storage systems in the presence of different fields, where the unit of the atom charge is one electron charge *e*.

Structure	Atom	$F = 0.000$ au		$F = +0.020$ au		$F = -0.020$ au	
		Before	After	Before	After	Before	After
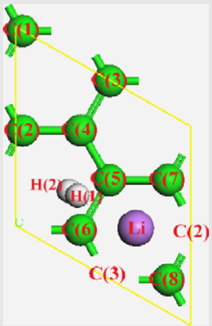	H(1)	0.000	−0.004	0.000	+0.054	0.000	−0.066
	H(2)	0.000	+0.001	0.000	+0.012	0.000	−0.066
	Li	+0.219	+0.262	+0.417	+0.334	+0.033	+0.128
	C(1)	−0.014	−0.015	−0.037	−0.034	+0.007	+0.014
	C(2)	−0.032	−0.036	−0.057	−0.054	−0.009	−0.002
	C(3)	−0.032	−0.042	−0.057	−0.055	−0.008	−0.005
	C(4)	−0.014	−0.015	−0.037	−0.034	+0.007	+0.014
	C(5)	−0.032	−0.037	−0.057	−0.056	−0.007	−0.005
	C(6)	−0.032	−0.037	−0.057	−0.056	−0.007	−0.005
	C(7)	−0.032	−0.042	−0.057	−0.055	−0.008	−0.005
	C(8)	−0.031	−0.035	−0.057	−0.054	−0.009	−0.002

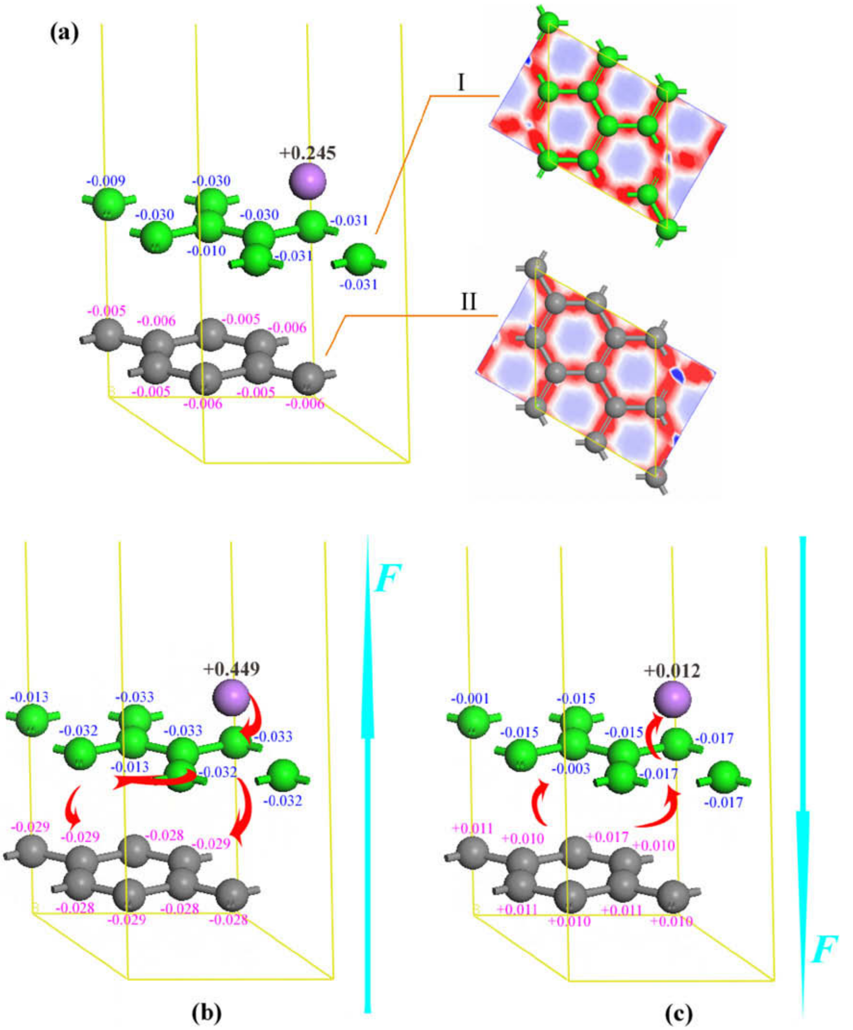

Fig. 3 – Hirshfeld charge analysis for the Li-doped bilayer graphene under: (a) $F = 0.000$ au, (b) $F = +0.020$ au, and (c) $F = -0.020$ au, where the red arrows indicate the possible charge transfer directions within these systems. In plot (a), insets I and II show the electron density difference for the upper and lower carbon layer, respectively. The red (or blue) region shows the location where the electron density has been enriched (or depleted). (For interpretation of the references to colour in this figure legend, the reader is referred to the web version of this article.)

shown in the insets of Fig. 3a, all carbon atoms in both sheets turn to red after doping, which indicates that the electron has been enriched in these areas.

On the basis of our results, it is apparent that charge redistribution occurs in the above system after superimposing an electric field. As shown in Fig. 3b, the charge carried by Li increases considerably from +0.245 to +0.449 *e* under a positive field. Partial electrons move from Li to the neighboring C ring. Interestingly, slight variations (0.001–0.003 *e*) can be observed in comparison with the C atoms shown in Fig. 3a. This is presumably because the electrons obtained from Li are not accumulated in this hexagonal ring, but will flow to the remaining C atoms in the same layer and the lower C sheet. This hypothesis is confirmed by the considerable charge variations in the second layer, where the charges of C atoms increase from −0.006 to −0.029 *e*, for example. Correspondingly, the E_{ad} value for the H_2/Li/bilayer graphene system decreases largely from −0.188 to −0.294 eV/H_2 when $F = +0.020$ au, as listed in Table 1. Similar binding enhancement can also be observed for the storage models in the case of 2 to 4H_2 molecules, although the variations are not as significant compared to the one-H system.

In contrast, electrons move upward from C to Li in the presence of a negative field. As shown in Fig. 3c, the carbon atoms in the upper layer remain anions but carry fewer negative charges when $F = -0.020$ au. Surprisingly, all C atoms in the lower layer become cations. Thus, the two layers may counteract each other and reduce the polar moments of the entire graphene. In addition, it is readily seen that the charge carried by Li becomes merely +0.012 *e*, which is much smaller than +0.245 *e* in the absence of field. Therefore, the negative field may significantly weaken the hydrogen adsorption. As listed in Table 1, the *E* values under −0.020 au field increase from −0.188, −0.244, −0.230, and −0.202 to −0.131, −0.105, −0.165, and −0.194 eV/H_2 for the 1 to 4H_2 on the Li-doped bilayer graphenes.

From the above discussion, we can conclude that the external electric field can be utilized as a switch to control the entire adsorption and desorption in the hydrogen storage systems, as proposed in our original hypothesis.

One may assume that, in addition to the field direction, the intensity of the fields may also be an essential parameter to adjust the effect of the switch. To check the validity of this hypothesis, Fig. 4 gives the intensity-dependent results for the $2H_2$/Li/bilayer graphene system, from which the binding strength is gradually enhanced when F increases from 0.000, +0.010, +0.015, to +0.020 au. In contrast, the E value increases from −0.159, −0.131, to −0.105 eV/H_2 when F changes from −0.010, −0.015, to −0.020 au. The average H–H bond length $d_{\text{H–H}}$ decreases as the positive intensity increases, whereas it increases as the negative intensity increases. Since the curve of $d_{\text{H–H}}(F)$ is inversely proportional to that of $-E_{\text{ad}}(F)$ (see Fig. 4), one can estimate the trends of hydrogen binding strength in terms of their corresponding bond length values. After full relaxation, entire systems are elongated even in the presence of upward or downward fields, which agrees with a prior result showing that clusters of particles are expanded along the direction of the field [46]. The rational is that although opposite electrostatic forces are superimposed, charge separation occurs which renders an elongation of the unconstrained system. Therefore, both the direction and the intensity of the external electric field play important roles in hydrogen storage systems.

To further understand the electronic hybridization, the DOS plots are analyzed for the single-layer and bilayer storage systems and depicted in Fig. 5. Three-layer and four-layer graphenes are also determined for comparison purposes. For the single-layer graphene, it is readily seen from Fig. 5a that the peaks of Li overlap with C in the lower energy range from −18.00 to −8.00 eV. Then, the main peak of Li-2s hybridizes with the σ bonding of the hydrogen molecule at −7.23 eV, which confirms the interaction between the dopant and the molecule. The neighboring three peaks of Li solely hybridize with C again at −5.84, −5.33, and −4.55 eV. All of the bands of H, Li, and C strongly overlap each other in the higher energy range. Similar hybridization behavior can be observed in the bilayer, three-layer and four-layer graphenes. Comparing the four plots in this figure, the main peak of H shifts left from −7.23 to −8.29, −8.64, and −8.83 eV in sequence, and overlap with their corresponding Li peaks. Although the orbitals of Li still hybridize with C below these main peaks, different from the single-layer graphene, H, Li, and C interact simultaneously in the energy range between the main peak and the Fermi level, as shown in Figs. 5b–d.

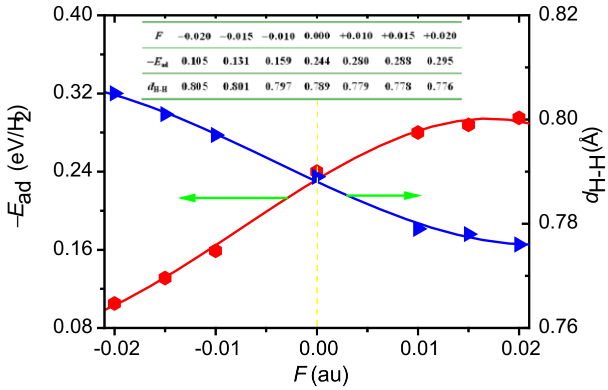

F	−0.020	−0.015	−0.010	0.000	+0.010	+0.015	+0.020
$-E_{\text{ad}}$	0.105	0.131	0.159	0.244	0.280	0.288	0.295
$d_{\text{H-H}}$	0.805	0.801	0.797	0.789	0.779	0.778	0.776

Fig. 4 – Intensity-dependent $-E_{\text{ad}}$ and $d_{\text{H–H}}$ results in the $2H_2$/Li/bilayer graphene system, where the discrete data are fitted by a third-order exponential function.

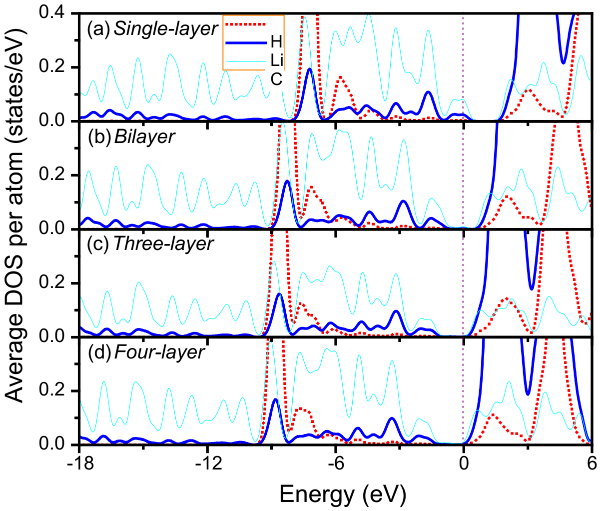

Fig. 5 – The DOS plots for H on Li-doped graphenes with different layers: (a) single-layer, (b) bilayer, (c) three-layer, and (d) four-layer. The Fermi level is set to zero and indicated by a dotted line.

Fig. 6 shows the intensity-dependent DOS plots for the $2H_2$/Li/bilayer graphene. We first address the hybridization situations for the system without field. Basically, the behavior illustrated in Fig. 6c is similar to that in Fig. 5b for the H_2/Li/bilayer graphene, namely that Li orbitals overlap with C in the lower energy range, whereas all Li, H, and C interact

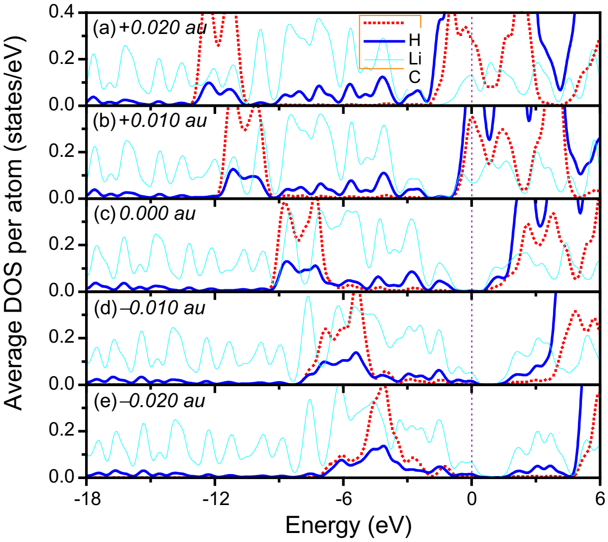

Fig. 6 – Intensity-dependent DOS plots for the $2H_2$/Li/bilayer graphene systems under different fields: (a) F = +0.020 au, (b) F = +0.010 au, (c) F = 0.000 au, (d) F = −0.010 au, and (e) F = −0.020 au. The Fermi level is set to zero and indicated by a dotted line.

perfectly with each other in the higher energy range. Differing from one-H system in Fig. 5, there are two main Li peaks in Fig. 5c, which are located at −8.69 and −7.29 eV. This is presumably because two H molecules are adsorbed simultaneously. Fig. 6a and b represents the DOS plots in the presence of positive fields where the orbitals are quite similar to that under $F = 0.000$ au. If the plot in Fig. 6c is selected as a reference, the sharpest peak of Li shifts from −8.69 to −11.20 eV when $F = +0.010$ au, and further moves left to −12.28 eV when $F = +0.020$ au. In all cases, these peaks continue to be hybridized strongly with σ bonding of hydrogen. These DOS changes confirm the strong effect of Li dopants in the hydrogen storage systems, even under the presence of electric fields. Since the entire orbitals are shifted to lower energy ranges, the enhancement of the hydrogen binding in the presence of a positive field is confirmed. In contrast, the peaks under −0.010 and −0.020 au move toward the Fermi level and hybridize with the σ bonding of hydrogen at −5.45 and −4.10 eV, which reflect that the entire system becomes unstable in the presence of a negative field; consistent with the trends of our calculated E values.

4. Conclusions

In conclusion, DFT calculations with electric fields are employed to study the interactions between the hydrogen molecules and the Li-doped single-layer and bilayer graphenes. Since lower layers also participate in the charge redistribution, the bilayer graphene is found to have slightly larger hydrogen binding strength than that of the single-layer. When $F = +0.020$ au, 88% binding enhancement is achieved for H_2/Li/single-layer graphene, where the E value decreases considerably from −0.153 to −0.288 eV/H_2. When $F = -0.020$ au, on the contrary, more than 50% binding weakness can be observed for 2H on Li-doped single-layer and bilayer graphenes. The charge analysis indicates that all C atoms achieve electrons from Li, which may render extra dipole moments between graphenes and the Li dopant. The opposite charge transfer happens in the presence of a negative field, where all carbon atoms in the lower layer of the bilayer graphene become cations. Our calculated results show that both the direction and intensity of field play important roles to characterize the hydrogen storage ability of graphenes.

Acknowledgements

Liu and Jiang acknowledge the financial support from the National Key Basic Research and Development Program of China (Grant No. 2010CB631001). Zhao, Nguyen, Li, and Lavernia would like to acknowledge support by the Office of Naval Research of the USA (Grant No. N00014-08-1-0405) with Dr. Lawrence Kabacoff as program officer.

REFERENCES

[1] Liu C, Fan YY, Liu M, Cong HT, Cheng HM, Dresselhaus MS. Hydrogen storage in single-walled carbon nanotubes at room temperature. Science 1999;286(5442):1127–9.
[2] Morris RE, Wheatley PS. Gas storage in nanoporous materials. Angew Chem, Int Ed 2008;47(27):4966–81.
[3] Meng S, Kaxiras E, Zhang ZY. Metal-diboride nanotubes as high-capacity hydrogen storage media. Nano Lett 2007;7(3):663–97.
[4] Siegel DJ, Wolverton C, Ozoliņš V. Thermodynamic guidelines for the prediction of hydrogen storage reactions and their application to destabilized hydride mixtures. Phys Rev B 2007;76(13):134102.
[5] Dillon AC, Heben MJ. Hydrogen storage using carbon adsorbents: past, present and future. Appl Phys A: Mater Sci Process 2001;72(2):133–42.
[6] Oostinga JB, Heersche HB, Liu XL, Morpurgo AF, Vandersypen LMK. Gate-induced insulating state in bilayer graphene devices. Nature Mater 2008;7(2):151–7.
[7] Geim AK, Novoselov KS. The rise of graphene. Nature Mater 2007;6(3):183–91.
[8] Lherbier A, Blase X, Niquet YM, Triozon F, Roche S. Charge transport in chemically doped 2D graphene. Phys Rev Lett 2008;101(3):036808.
[9] Schlapbach L, Zuttel A. Hydrogen-storage materials for mobile applications. Nature 2001;414(6861):353–8.
[10] Novoselov KS, Geim AK, Morozov SV, Jiang D, Zhang Y, Dubonos SV, et al. Electric field effect in atomically thin carbon films. Science 2004;306(5296):666–9.
[11] Patchkovskii S, Tse JS, Yurchenko SN, Zhechkov L, Heine T, Seifert G. Graphene nanostructures as tunable storage media for molecular hydrogen. Proc Natl Acad Sci USA 2005;102(30):10439–44.
[12] Durgun E, Ciraci S, Yildirim T. Functionalization of carbon-based nanostructures with light transition-metal atoms for hydrogen storage. Phys Rev B 2008;77(8):2085405-1–92.
[13] Roman T, Dino WA, Nakanishi H, Kasai H, Sugimoto T, Tange K. Hydrogen pairing on graphene. Carbon 2007;45(1):218–20.
[14] Boukhvalov DW, Katsnelson MI, Lichtenstein AI. Hydrogen on graphene: electronic structure, total energy, structural distortions and magnetism from first-principles calculations. Phys Rev B 2008;77(3):2035427-1–72.
[15] Duplock EJ, Scheffler M, Lindan PJD. Hallmark of perfect graphene. Phys Rev Lett 2004;92(22):2225502-1–42.
[16] Sha XW, Jackson B, Lemoine D. Quantum studies of Eley–Rideal reactions between H atoms on a graphite surface. J Chem Phys 2002;116(16):7158–69.
[17] Miwa RH, Martins TB, Fazzio A. Hydrogen adsorption on boron doped graphene: an ab initio study. Nanotechnology 2008;19(15):155708-1–7.
[18] Panella B, Hones K, Muller U, Trukhan N, Schubert M, Putter H, et al. Desorption studies of hydrogen in metal–organic frameworks. Angew Chem, Int Ed 2008;47(11):2138–42.
[19] Ferre-Vilaplana A. Storage of hydrogen adsorbed on alkali metal doped single-layer all-carbon materials. J Phys Chem C 2008;112(10):3998–4004.
[20] Cabria I, López MJ, Alonso JA. Enhancement of hydrogen physisorption on graphene and carbon nanotubes by Li doping. J Chem Phys 2005;123(20):204721-1–9.
[21] Henwood D, Carey JD. Ab initio investigation of molecular hydrogen physisorption on graphene and carbon nanotubes. Phys Rev B 2007;75(24):245413.
[22] Arellano JS, Molina LM, Rubio A, Alonso JA. Density functional study of adsorption of molecular hydrogen on graphene layers. J Chem Phys 2000;112(18):8114–9.
[23] Rojas MI, Leiva EPM. Density functional theory study of a graphene sheet modified with titanium in contact with different adsorbates. Phys Rev B 2007;76:2155415-1–82.
[24] Ataca C, Aktürk E, Ciraci S, Ustunel H. High-capacity hydrogen storage by metallized graphene. Appl Phys Lett 2008;93(4):043123.

[25] Dimitrakakis GK, Tylianakis E, Froudakis GE. Pillared graphene: a new 3-D network nanostructure for enhanced hydrogen storage. Nano Lett 2008;8(10):3166–70.

[26] Froudakis GE. Why alkali-metal-doped carbon nanotubes possess high hydrogen uptake. Nano Lett 2001;1(10):531–3.

[27] Ahn CH, Bhattacharya A, Di Ventra M, Eckstein JN, Frisbie CD, Gershenson ME, et al. Electrostatic modification of novel materials. Rev Mod Phys 2006;78:1185–212.

[28] Qiao L, Zheng WT, Wen QB, Jiang Q. First-principles density-functional investigation of the effect of water on the field emission of carbon nanotubes. Nanotechnology 2007;18(15):155707-1–6.

[29] Tomonari M, Sugino O. DFT calculation of vibrational frequency of hydrogen atoms on Pt electrodes: analysis of the electric field dependence of the Pt–H stretching frequency. Chem Phys Lett 2007;437(4–6):170–5.

[30] Migani A, Sousa C, Sanz F, Illas F. Electric field induced electron transfer at the adsorbate–surface interface. Effect of the type of metal surface. Phys Chem Chem Phys 2005;7(18):3353–8.

[31] Lin YM, Avouris P. Strong suppression of electrical noise in bilayer graphene nanodevices. Nano Lett 2008;8(8):2119–25.

[32] Castro EV, Novoselov KS, Morozov SV, Peres NMR, Dos Santos J, Nilsson J, et al. Biased bilayer graphene: semiconductor with a gap tunable by the electric field effect. Phys Rev Lett 2007;99:216802.

[33] Ohta T, Bostwick A, Seyller T, Horn K, Rotenberg E. Controlling the electronic structure of bilayer graphene. Science 2006;313(5789):951–4.

[34] Delley B. An all-electron numerical-method for solving the local density functional for polyatomic-molecules. J Chem Phys 1990;92(1):508–17.

[35] Delley B. From molecules to solids with the DMol^3 approach. J Chem Phys 2000;113(18):7756–64.

[36] Perdew JP, Wang Y. Accurate and simple analytic representation of the electron-gas correlation-energy. Phys Rev B 1992;45(23):13244–9.

[37] de Andres PL, Ramírez R, Vergés JA. Strong covalent bonding between two graphene layers. Phys Rev B 2008;77:2045403-1–52.

[38] Yoon M, Yang SY, Wang E, Zhang ZY. Charged fullerenes as high-capacity hydrogen storage media. Nano Lett 2007;7(9):2578–83.

[39] Yang RT. Hydrogen storage by alkali-doped carbon nanotubes-revisited. Carbon 2000;38(4):623–6.

[40] Zhu ZH, Lu GQ, Smith SC. Comparative study of hydrogen storage in Li- and K-doped carbon materials – theoretically revisited. Carbon 2004;42(12–13):2509–14.

[41] Perdew JP, Chevary JA, Vosko SH, Jackson KA, Pederson MR, Singh DJ, et al. Atoms, molecules, solids, and surfaces: applications of the generalized gradient approximation for exchange and correlation. Phys Rev B 1992;46(11): 6671–87.

[42] Tada K, Furuya S, Watanabe K. Ab initio study of hydrogen adsorption to single-walled carbon nanotubes. Phys Rev B 2001;63(15):155405-1–4.

[43] González S, Sousa C, Illas F. Electric field effects in the chemisorption of CO on bimetallic RhCu surface models. Surf Sci 2004;548(1–3):209–19.

[44] Li J, Furuta T, Goto H, Ohashi T, Fujiwara Y, Yip S. Theoretical evaluation of hydrogen storage capacity in pure carbon nanostructures. J Chem Phys 2003;119(4):2376–85.

[45] Gülseren O, Yildirim T, Ciraci S. Tunable adsorption on carbon nanotubes. Phys Rev Lett 2001;87(11):2116802-1–42.

[46] Aertsens M, Naudts J. Field-induced percolation in a polarized lattice gas. J Stat Phys 1991;62(3–4):609–30.